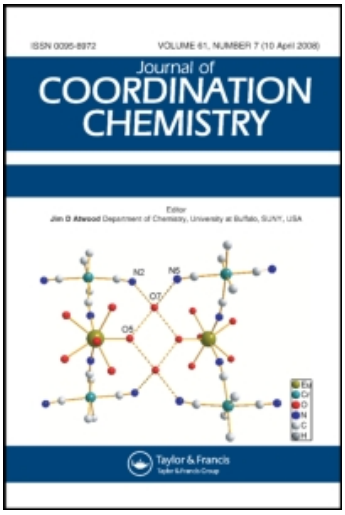

Journal of Coordination Chemistry
Publication details, including instructions for authors and subscription information:
http://www.informaworld.com/smpp/title~content=t713455674

Crystal structures and luminescence properties of two new terbium complexes with aromatic carboxylic acid

Ying-Xia Zhou[a]; Xiao-Qing Shen[a]; Hong-Yun Zhang[a]; Chen-Xia Du[a]; Ben-Lai Wu[a]; Hong-Wei Hou[a]
[a] Department of Chemistry, Zhengzhou University, Zhengzhou, P.R. China

To cite this Article Zhou, Ying-Xia , Shen, Xiao-Qing , Zhang, Hong-Yun , Du, Chen-Xia , Wu, Ben-Lai and Hou, Hong-Wei(2008) 'Crystal structures and luminescence properties of two new terbium complexes with aromatic carboxylic acid', Journal of Coordination Chemistry, 61: 24, 3981 — 3992
To link to this Article: DOI: 10.1080/00958970802192233
URL: http://dx.doi.org/10.1080/00958970802192233

Journal of Coordination Chemistry
Vol. 61, No. 24, 20 December 2008, 3981–3992

Taylor & Francis
Taylor & Francis Group

Crystal structures and luminescence properties of two new terbium complexes with aromatic carboxylic acid

YING-XIA ZHOU, XIAO-QING SHEN, HONG-YUN ZHANG*, CHEN-XIA DU, BEN-LAI WU and HONG-WEI HOU

Department of Chemistry, Zhengzhou University, Zhengzhou, 450052, P.R. China

(*Received 17 November 2007; in final form 5 March 2008*)

Two new terbium complexes with aromatic carboxylic acids, $[(Tb)_2(L_1)_6(H_2O)_4]$ (**1**) and $[(Tb)_2(L_2)_6(H_2O)_2(DMF)_2]$ (**2**) (HL_1: nicotinic acid; HL_2: 4-hydroxybenzoic acid), with different coordination geometries have been synthesized and their crystal structures determined. The luminescence properties of the two complexes, including the phosphorescence lifetime, have been investigated. The effect of a secondary ligand on luminescence of the ternary terbium complex with carboxylic acid and the relationship between luminescence properties and crystal structure, including coordination mode of the carboxyl groups from HL_1 and HL_2 and coordination mode of a secondary ligand, are discussed.

Keywords: Terbium; Nicotinic acid; 4-Hydroxybenzoic acid; Crystal structure; Luminescence

1. Introduction

Rare earth complexes that emit are of interest for applications in biochemistry, material chemistry and medicine [1]. For instance, rare earth metal complexes with carboxylic acids may be used as structural and functional probes of biological macromolecules [2, 3]. Therefore, many rare earth metal carboxylate complexes have been synthesized and the relationship between fluorescence properties and structures have been studied [4–24]. Lanthanide complexes with aromatic carboxylic acids readily form dimeric or infinite chain polymeric structures with higher thermal or luminescent stabilities than other lanthanide complexes due to bridging carboxylate ligands in various coordination modes. Effects of a second ligand in ternary rare earth metal complexes on luminescence intensity have been studied, and the energy transfer mechanism has been discussed [19–24]. Little research has been done on crystal structures of rare earth metal complexes with aromatic carboxylic acids, such as hydroxybenzoic acid, except several papers on composition and properties of solid ternary 4-hydroxybenzoic acid complexes with lanthanide ions [25–28]. Pyridyl carboxylic acids are heterocyclic carboxylic acids with conjugated structures. Molecular structures for some lanthanide complexes with pyridyl carboxylic acids have been discussed, but their luminescence properties are less investigated [29–32].

*Corresponding author. Email: wzhy917@zzu.edu.cn

Journal of Coordination Chemistry
ISSN 0095-8972 print/ISSN 1029-0389 online
DOI: 10.1080/00958970802192233

In this article, syntheses, crystal structures and the photophysical properties of $[(Tb)_2(L_1)_6(H_2O)_4]$ (**1**) and $[(Tb)_2(L_2)_6(H_2O)_2(DMF)_2]$ (**2**) are reported. The effect of a second ligand on luminescence and the relationship between the luminescence and coordination mode of the ligand are also discussed.

2. Experimental

2.1. *Chemicals and physical measurements*

All chemicals were of reagent grade, and most were purchased from Zhengzhou Zhongliang Chemical Reagent Company, and used without purification. $TbCl_3 \cdot 6H_2O$ was prepared by treating terbium oxide (Tb_4O_7) with concentrated hydrochloric acid according to the conventional method [33].

Single crystal structures were measured on a Rigaku-Raxis-IV X-ray diffractometer. Thermal analyses were done with a MKV thermal analyzer in air from room temperature to 650°C. IR spectra were recorded on a FTS-40 infrared spectrophotometer as KBr pellets in the range 4000–400 cm^{-1}. Ultraviolet absorption spectra were measured using an Agilent 8453 spectrophotometer. The luminescence (excitation and emission) spectra for powdered samples were determined with a Fluoro Max-p spectrophotometer at room temperature: excitation wavelength = 350 nm, delay time = 0.01 ms, scan speed = 1000 nm s^{-1}, excitation and emission slit width = 1.0 nm, and the phosphorescence lifetimes were measured with an excitation wavelength of 545 nm.

2.2. *Syntheses of the complexes*

2.2.1. Synthesis of $[(Tb)_2(L_1)_6(H_2O)_4]$ (1). To 10 mL aqueous solution of $TbCl_3 \cdot 6H_2O$ (0.3734 g, 1.0 mmol), a solution of nicotinic acid (0.369 g, 3.0 mmol) in a minimum of methanol was slowly added under stirring at room temperature. The pH of the mixed solution was adjusted to 6.0 with dilute aqueous ammonia and stirred for 2 h, when white precipitate appeared. The resulting solution was filtered and the filtrate allowed to slowly evaporate at room temperature. After 3 months, well-shaped colorless single crystals of **1** suitable for X-ray diffraction analysis were obtained. Yield was 58%. IR (KBr, cm^{-1}): 1548($\nu_s COO^-$) s, 1413($\nu_{as} COO^-$) s.

2.2.2. Synthesis of $[(Tb)_2(L_2)_6(H_2O)_2(DMF)_2]$ (2). The synthesis procedure for **2** is similar to that of **1** except that ethanol is used to dissolve 4-hydroxybenzoic acid. Colorless crystals of **2** suitable for single-crystal X-ray diffraction were obtained after 4 months. Yield for **2** was 39%. IR (KBr, cm^{-1}): 1597($\nu_s COO^-$) s, 1420($\nu_{as} COO^-$) s, 3389($\nu_s HO^-$) m.

2.3. *Crystal data collection and refinement*

Intensity data of **1** and **2** were measured with a Rigaku-Raxis-IV X-ray diffractometer using monochromated Mo-Kα ($\lambda = 0.71073$ Å) radiation at 291(2) K

for **1** and 293(2) K for **2**. 6958 reflections were measured over the ranges $2.08 \le 2\theta \le 26.50$, $0 \le h \le 12$, $-14 \le k \le 14$, $-22 \le l \le 22$, yielding 3975 unique reflections for **1**. For **2**, 5057 reflections were measured over the ranges $1.59 \le 2\theta \le 26.49$, $0 \le h \le 14$, $0 \le k \le 10$, $-32 \le l \le 32$, yielding 5057 unique reflections. Raw data were corrected and the structures were solved using SHELX-97. All non-hydrogen atoms were refined anisotropically by full-matrix least-squares. Hydrogen atoms including the water hydrogen atoms were added geometrically and not refined. Full-matrix least-squares calculation on F^2 were applied on the final refinement. The refinement converged at $R_1 = 0.0379$ and $wR_2 = 0.0969$ for reflections with $I > 2\sigma(I)$ for **1**, and $R_1 = 0.0349$ and $wR_2 = 0.0994$ for reflections with $I > 2\sigma(I)$ for **2**. Maximum and minimum peaks in the final difference maps were 1.077 and $-1.029\,e\,Å^3$ for **1** and 0.936 and $-1.099\,e\,Å^3$ for **2**. Details of the crystal structural determinations are summarized in table 1. Full atomic data are available as a file in CIF format.

3. Results and discussion

3.1. *Thermal analysis*

TG-DTA analyses reveal that **1** and **2** begin to lose their weight due to thermal decomposition at 185°C and 110°C, respectively. The thermal decomposition for both complexes is complete at 650°C. Complex **1** lost its two coordinated water molecules from 185–230°C (loss of weight found: 6.1%; loss of weight calculated based on the loss of two water molecules: 6.4%). The weight loss of **1** from 395–600°C is assigned to the loss of one chelated nicotinic acid anion (observed, 23.2%; calculated, 21.7%).

Table 1. Crystal data and structure refinement parameters for **1** and **2**.

	$[(Tb)_2(L_1)_6(H_2O)_4]$ (**1**)	$[(Tb)_2(L_2)_6(H_2O)_2(DMF)_2]$ (**2**)
Formula	$C_{18}H_{12}N_3O_8Tb$	$C_{24}H_{21}NO_{11}Tb$
M	557.23	658.34
Crystal system	Monoclinic	Monoclinic
Space group	*P*2(1)/*c*	*P*2(1)/*c*
Unit cells and dimensions (Å, °)		
a	9.6614(19)	11.612(2)
b	11.772(2)	8.7172(17)
c	17.767(4)	25.820(5)
α	90.00	90.00
β	91.97(3)	97.92(3)
γ	90.00	90.00
V (Å^3)	2019.6(7)	2588.7(9)
D_{Calcd} (Mg m^{-3})	1.833	1.689
Z	4	4
μ (mm^{-1})	3.552	2.792
Reflections collected/unique	6958/3975	5057/5057
Data/restraints/parameters	3975/0/272	5057/0/335
R_1	0.0379	0.0349
wR_2	0.0969	0.0994
Goodness-of-fit on F^2	1.048	1.054
$\Delta\rho_{min.}$ and $\Delta\rho_{max.}$ (e Å^{-3})	1.077 and −1.029	0.936 and −1.099

Complex **2** quickly lost coordinated water molecule in the temperature range 110–180°C (found, 3.0%; calculated, 2.7%). The weight loss of **2** from 200–260°C is assigned to loss of one DMF (observed, 10.3%; calculated, 11.1%) and from 365–600°C is assigned to loss of two chelated 4-hydroxybenzoic acid anions (observed, 38.0%; calculated, 41.5%). The results suggest that **1** is more stable than **2**, possibly from more bridged carboxylates in **1** than **2**. These results are consistent with the bond length comparisons from the structural analysis discussed below. The Tb–O (bridged carboxylate) bond length is the shortest among all the Tb–O bond lengths (see table 2).

3.2. *Description of crystal structures*

3.2.1. Crystal structure of 1. The crystal structure parameters and bond lengths and bond angles of **1** are listed in tables 1 and 2, respectively. The coordination geometry and atom labeling in the crystal structure of **1** are shown in figure 1, with hydrogen atoms omitted for clarity. Complex **1** belongs to the monoclinic system with space

Table 2. Selected bond distances (Å) and angles (°) for **1** and **2**.

Complex **1**		Complex **2**	
Bond distances		Bond distances	
Tb(1)–O(6)#1	2.353(4)	Tb(1)–O(7)	2.286(3)
Tb(1)–O(3)	2.358(3)	Tb(1)–O(8)#1	2.336(3)
Tb(1)–O(4)#1	2.379(3)	Tb(1)–O(11)	2.347(3)
Tb(1)–O(5)	2.396(4)	Tb(1)–O(4)	2.390(3)
Tb(1)–O(8)	2.422(4)	Tb(1)–O(10)	2.391(3)
Tb(1)–O(7)	2.440(4)	Tb(1)–O(1)	2.404(3)
Tb(1)–O(2)	2.486(4)	Tb(1)–O(5)	2.496(3)
Tb(1)–O(1)	2.555(4)	Tb(1)–O(2)	2.599(3)
Angles		Angles	
O(6)#1–Tb(1)–O(3)	73.63(17)	O(7)–Tb(1)–O(8)#1	114.20(13)
O(3)–Tb(1)–O(4)#1	126.69(13)	O(7)–Tb(1)–O(11)	155.85(14)
O(3)–Tb(1)–O(5)	85.38(16)	O(7)–Tb(1)–O(4)	91.03(13)
O(4)#1–Tb(1)–O(5)	75.45(16)	O(11)–Tb(1)–O(4)	88.49(13)
O(3)–Tb(1)–O(8)	145.05(14)	O(7)–Tb(1)–O(10)	80.01(13)
O(5)–Tb(1)–O(8)	76.00(15)	O(11)–Tb(1)–O(10)	81.73(14)
O(3)–Tb(1)–O(7)	73.87(14)	O(4)–Tb(1)–O(10)	129.51(12)
O(5)–Tb(1)–O(7)	74.38(15)	O(7)–Tb(1)–O(1)	72.89(12)
O(8)–Tb(1)–O(7)	72.76(13)	O(4)–Tb(1)–O(1)	85.75(12)
O(6)#1–Tb(1)–O(2)	86.65(16)	O(10)–Tb(1)–O(1)	135.86(11)
O(3)–Tb(1)–O(2)	84.36(13)	O(7)–Tb(1)–O(5)	85.38(12)
O(4)#1–Tb(1)–O(2)	136.24(13)	O(4)–Tb(1)–O(5)	53.41(11)
O(5)–Tb(1)–O(2)	144.29(15)	O(1)–Tb(1)–O(5)	133.52(12)
O(7)–Tb(1)–O(2)	69.92(13)	O(7)–Tb(1)–O(2)	121.93(11)
O(3)–Tb(1)–O(1)	127.34(14)	O(4)–Tb(1)–O(2)	70.63(11)
O(5)–Tb(1)–O(1)	147.15(15)	O(10)–Tb(1)–O(2)	152.63(12)
O(7)–Tb(1)–O(1)	108.86(14)	O(1)–Tb(1)–O(2)	51.85(10)
O(2)–Tb(1)–O(1)	51.79(12)	O(5)–Tb(1)–O(2)	118.44(11)
Hydrogen bond distances		Hydrogen bond distances	
O8–H···N2	2.761 Å	O10–H···O5	2.766 Å
O8–H···N3	2.864 Å	O10–H···O1	2.815 Å
O7–H···N1	2.768 Å	O5–H···O6	2.811 Å
O7–H···O2	2.781 Å	O6–H···O2	3.005 Å

Symmetry transformations used to generate equivalent atoms: #1:$-x, -y, -z$.

group $P2(1)/c$, with a dimeric formula $[(Tb)_2(L_1)_6(H_2O)_4]$ with two equivalent structural units corresponding to one half of the dimer related by a crystallographic inversion center, similar to $[Sm(5\text{-Brnic})_3(H_2O)_2 \cdot H_2O]$ [29]. There are two coordination modes of nicotinic acid anions in **1**: (a) bidentate-bridging with two Tb ions connected into a dimeric structure by a bridging carboxylate from a nicotinic acid anion; (b) bidentate-chelating with two oxygens of a carboxylate from a nicotinic acid anion coordinated to the same Tb^{3+}. In $[(Tb)_2(L_1)_6(H_2O)_4]$, two symmetrical Tb^{3+} ions are bridged by four nicotinic acid anions with each Tb^{3+} eight-coordinate with six oxygens from five nicotinic acids (L_1) and two oxygens from coordinated water. The coordination sphere around Tb^{3+} can be described as a distorted square antiprism. Bond lengths between the Tb(1) and four oxygen atoms (O(3), O(5), O(4A) and O(6A)) from four bridged nicotinic acid anions are in the range 2.353(4)–2.396(4) Å, bond lengths of Tb(1) with O(1) and O(2) from a chelated nicotinic acid anion are 2.555(4) Å (Tb(1)–O(1)) and 2.486(4) Å (Tb(1)–O(2)). Bond distances of Tb(1) with oxygens with bridging coordination are shorter than those by chelating. In addition, bond distances of Tb(1) with two oxygens of water are 2.440(4) Å (Tb(1)–O(7)) and 2.422(4) Å (Tb(1)–O(8)), shorter than those of chelated nicotinic acid anion, but longer than those with bridging coordination. The eight Tb–O distances are close to literature values [29]. The bond angle of Tb and oxygens of chelated nicotinic acid anions is 51.79(12)° (O(1)–Tb(1)–O(2)).

The packing of a unit cell for **1** are shown in figure 2. Two kinds of intermolecular hydrogen bonds exist in **1**. Hydrogen bonds between coordinated water and nitrogen on pyridine of the bridging and chelating nicotinic acid from adjacent structural units are O8–H···N2 = 2.761 Å, O8–H···N3 = 2.864 Å and O7–H···N1 = 2.768 Å. Hydrogen bonds of coordinated water and oxygen of chelated carboxylate of nicotinic acid from adjacent structural units is O7–H···O2 = 2.781 Å. The structural units are connected

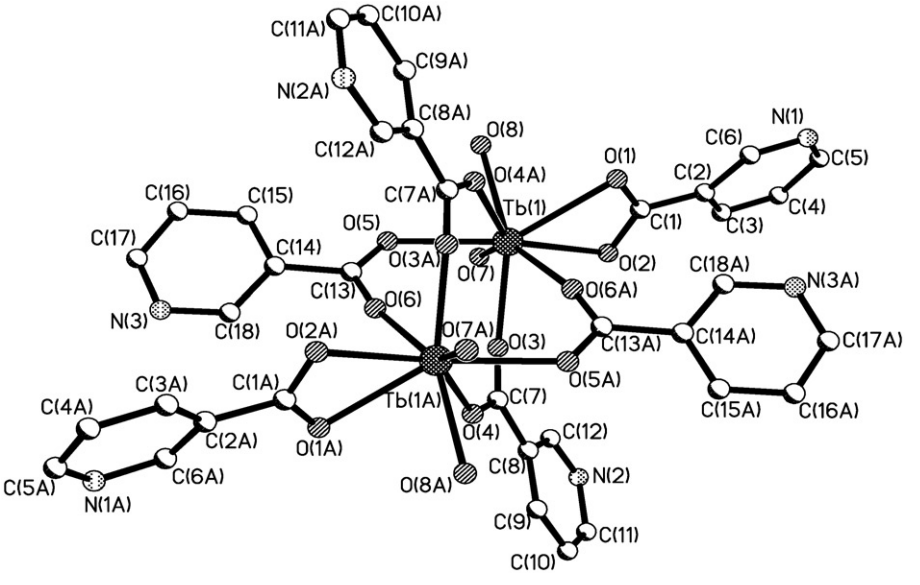

Figure 1. Structural unit for $[(Tb)_2(L_1)_6(H_2O)_4]$.

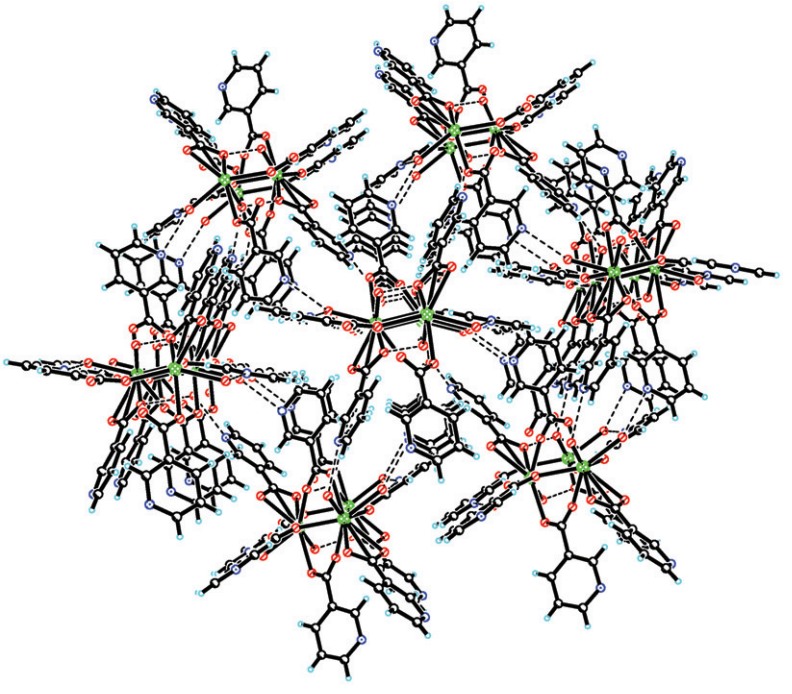

Figure 2. Packing view of the unit cell for **1**.

into a 1-D chain along *a* by O7–H···O2 hydrogen bond and the 1-D chains are linked with adjacent chains by O8–H···N2, O8–H···N3 and O7–H···N1 hydrogen bonds to expand into a 3-D supramolecular complex, stabilizing the network structure of **1**.

3.2.2. Crystal structure of 2. As shown in table 1 and figure 3, the crystal structure of **2** belongs to the monoclinic system with space group $P2(1)/c$ in a binuclear molecule $[(Tb)_2(L_2)_6(H_2O)_2(DMF)_2]$ with two equivalent structural units corresponding to one half of the dimer. There are two coordination modes for 4-hydroxybenzoic acid: bidentate-bridging and bidentate-chelating, similar to **1**. The two symmetrical Tb^{3+} ions are bridged by two 4-hydroxybenzoates; each Tb^{3+} center is additionally chelated by two carboxylates from two 4-hydroxybenzoic acids, one H_2O and one DMF. The eight oxygens surrounding Tb^{3+} form a distorted square-antiprism. The crystal structure of **2** is different from **1** in spite of similar reaction conditions, but similar to the literature [20]. This difference can be attributed to the space effect of DMF and H_2O. The bond distances between Tb(1) and O(7) and O(8A) from two bridged 4-hydroxybenzoic acids are 2.286(3) Å and 2.336(3) Å, respectively. The bond distances of O(1), O(2), O(4) and O(5) from two chelated 4-hydroxybenzoic acids with Tb(1) are in the range 2.390(3)–2.599(3) Å, all longer than for bridged coordination. The Tb–O(10) and Tb–O(11) bond distances of H_2O and DMF, respectively, are 2.391(3) Å and 2.347(3) Å, respectively, shorter than those of chelate coordination but longer than those of bridge coordination. The bond angles of Tb ion and the two oxygens of chelated 4-hydroxybenzoic acid are 51.85(10)° (O(1)–Tb(1)–O(2)) and 53.41(11)° (O(4)–Tb(1)–O(5)), respectively. Detailed data of selected bond distances and bond angles for **2** are shown in table 2.

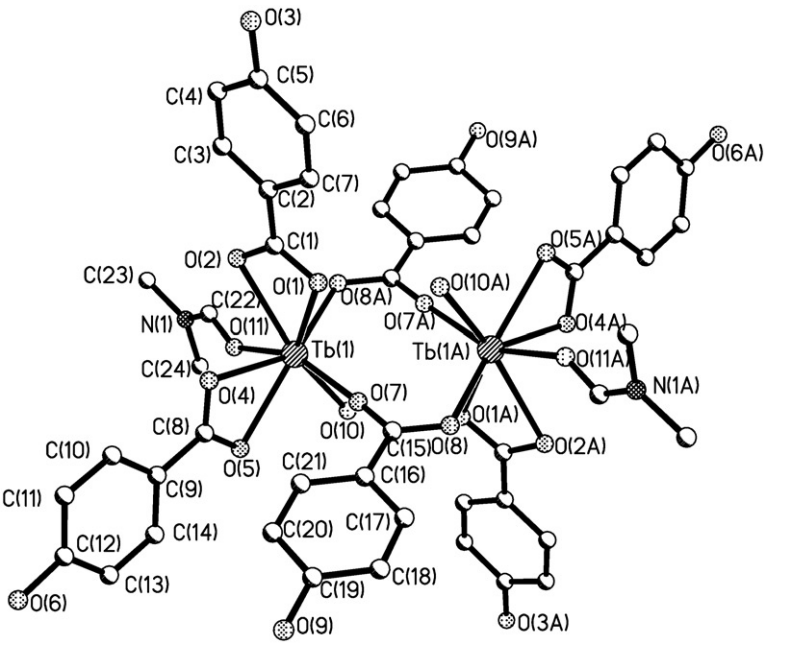

Figure 3. Structural unit drawing of **2**.

In the crystal structure of **2** there are complicated hydrogen bonds, the intramolecular hydrogen bond of the coordinated water and oxygen of chelating carboxyl from 4-hydroxybenzoic acid O10–H $\cdots$ O5 = 2.766 Å, and the intermolecular hydrogen bond of the coordinated water and oxygen of chelated carboxyl of 4-hydroxybenzoic acid from adjacent structural units, O10–H $\cdots$ O1 = 2.815 Å. Another intermolecular hydrogen bond from hydroxyl of 4-hydroxybenzoic acid and hydroxyl oxygen of 4-hydroxybenzoic acid from adjacent structural units is O5–H $\cdots$ O6 = 2.811 Å. The third intermolecular hydrogen bond from hydroxyl of 4-hydroxybenzoic acid and chelated oxygen of 4-hydroxybenzoic acid from adjacent structural units is O6–H $\cdots$ O2 = 3.005 Å. The structural units are linked into a 1-D chain along *b* by the intermolecular hydrogen O10–H $\cdots$ O1 and 1-D chains link with adjacent chains along different directions by O5–H $\cdots$ O6 and O6–H $\cdots$ O2 hydrogen bonds constructing the 3-D framework. Packing view of the unit cell for $[(Tb)_2(L_2)_6(H_2O)_2(DMF)_2]$ is shown in figure 4.

Comparing $[Tb(L)_3(DMSO)(H_2O)]_2$ and $[Tb(L)_3(DMF)(H_2O)]_2$ with complex $[Tb(L)_3(H_2O)_2]_2 \cdot 2H_2O$ [4] (HL = p-aminobenzoic acid), Oyang *et al.* [20] found that coordination water can be replaced with DMSO, DMF or other solvent, giving different crystal structures. The coordination geometry of **1** is distinct from that of **2**, where coordination water in **1** was replaced by DMF, which results in different structures. This difference can be attributed to the space effect [20].

Complexes of middle-lanthanide ions (Tb^{3+}–Er^{3+}) with *p*-aminobenzoic acid have two-dimensional (2-D) array structures when the N atoms of amino groups can be coordinated to the metal, and possess binuclear structures when the N atoms are uncoordinated [4, 34]. Complexes **1** and **2** are binuclear structures, consistent with

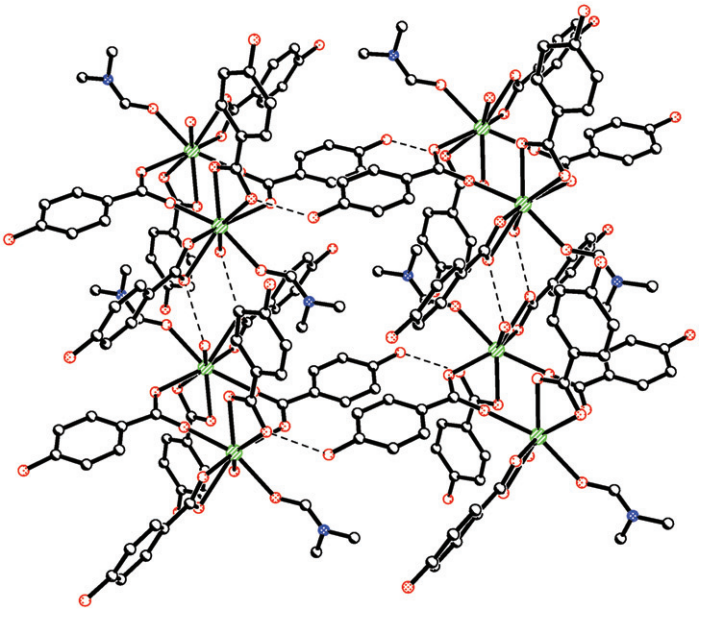

Figure 4. Packing view of the unit cell for **2**.

the literature. For **1**, four carboxylates from four nicotinic acids bridge two Tb^{3+} forming a dimer and steric effects prevent coordination of pyridine; thus **1** is a dimer. For **2**, hydroxy group from p-aminobenzoic acid does not deprotonate and **2** is also a dimer.

3.3. *Photophysical properties*

3.3.1. UV spectra. Figure 5 shows the ultraviolet–visible absorption spectra for ligands (HL_1 and HL_2) and their complexes (**1** and **2**) (5.0×10^{-5} mol L^{-1} in methanol). They all exhibit absorption peaks from 200–300 nm with maximum absorptions at 210–220 nm and 250–270 nm, attributed to $n \rightarrow \pi^*$ and $\pi \rightarrow \pi^*$ transitions of pyridine from HL_1 and phenyl from HL_2. Compared with the free HL_1, the characteristic absorption band of **1** is red-shifted, while it is blue-shifted for **2** compared with free HL_2 (table 3). There are four bridging carboxylates in **1** compared to two in **2**. The conjugated system of **1** is expanded due to each bridging carboxylate connecting two terbium ions, leading to energy reduction for $n \rightarrow \pi^*$ and $\pi \rightarrow \pi^*$ transitions [31]. Electron cloud excursion from the pyridine ring or benzene ring to Tb^{3+} occurs easily through chelated carboxylate since Tb^{3+} is almost in the plane of pyridine or benzene, causing blue shift of $\pi \rightarrow \pi^*$ transition [35].

3.3.2. Luminescence property. As discussed in section 3.3.1, ultraviolet absorption peaks of **1** and **2** can be attributed to characteristic absorptions of HL_1 and HL_2, indicating that HL_1 and HL_2 are the energy donors and luminescence sensitizers of Tb^{3+}.

The emission spectra (see figure 6) at excitation wavelengths (λ_{ex}) 350 nm and the phosphorescence lifetime for **1** and **2** are obtained. There are four spectral bands at

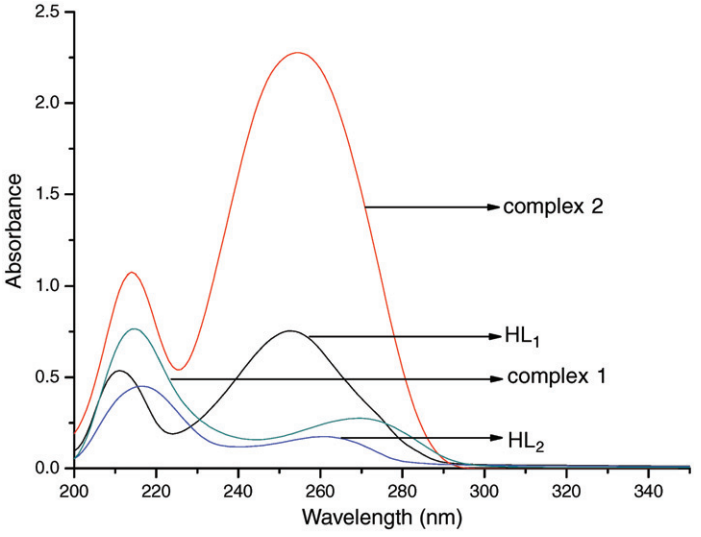

Figure 5. UV absorption spectra of HL_1 and HL_2 and **1** and **2** in methanol with concentrations of 5.0×10^{-5} mol L^{-1}.

Table 3. UV spectral data of HL_1, HL_2, **1** and **2** in methanol at 5.0×10^{-5} mol L^1.

Compound	λ (nm) (ε (L mol^{-1} cm^{-1}))	λ (nm) (ε (L mol^{-1}cm^{-1}))
HL_1	211 (1.095×10^4)	253 (1.515×10^4)
Complex **1**	216 (1.744×10^4)	269 (6.373×10^3)
HL_2	217 (9.119×10^3)	263 (3.578×10^3)
Complex **2**	216 (2.635×10^4)	259 (4.857×10^4)

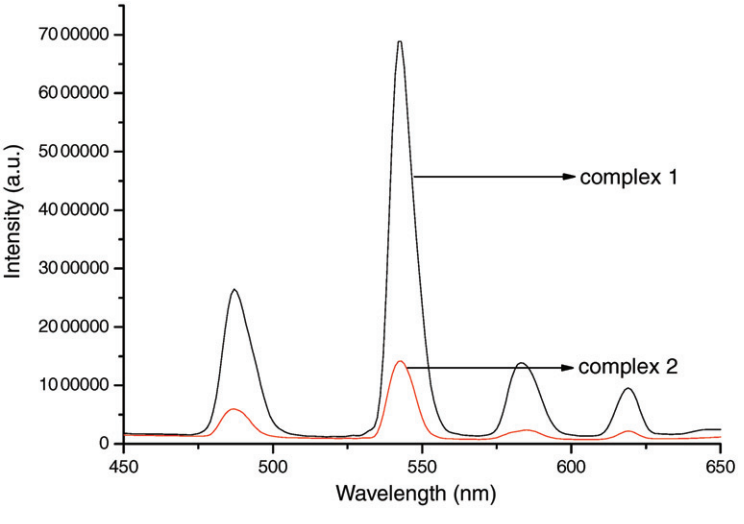

Figure 6. Emission spectra of **1** and **2**.

emission wavelengths (λ_{ex}) ca 489, 545, 585 and 620 nm in the emission spectra which correspond to the $^5D_4$-$^7F_6$, $^5D_4$-$^7F_5$, $^5D_4$-$^7F_4$ and $^5D_4$-$^7F_3$ transitions of Tb^{3+}, respectively; the relative intensity of the band at 545 nm is the most intense. The fluorescence intensity (7750380) of **1** is stronger than that (1232980) of **2**, and **1** displays longer phosphorescence lifetime (2.69 ms) than **2** (2.22 ms). The luminescence performance of **1** is better than that of **2**, although **1** has two coordinated water molecules around Tb^{3+} ion and **2** has only one. Generally [1], coordination of water decreases the luminescence intensity of a rare earth complex because the thermal vibration of water consumes partially the energy absorbed. The unusual result from our experiments indicates that the structure of a complex, including ligand coordination and the characteristics of the second ligand, could influence luminescence.

Yu and Su studied photoacoustic amplitude spectra and luminescence spectra of $Tb(Benz)_3$, $Tb(Benz)_3(Phen)$ and $Tb(Benz)_3(Bpy)$ [19] and suggested that an energy gap exists between the triplet state of the ligand and the resonance level of the rare earth ion. Part of the energy absorbed by Benz may be transferred to the second ligand (e.g. Phen) before being transferred to Tb^{3+}. However, the energy gap is so small that the inverse energy transfer rate from the thermally activated Tb^{3+} to the second ligand (Phen) increases even more, making the luminescence intensity of $Tb(Benz)_3(Phen)$ the lowest. According to Yu and Su, the energy gap between the triplet state of HL_1 and the resonance level of the Tb^{3+} ion may be suitable for energy transfer from the ligand L_1^- to Tb^{3+} without a second ligand in **1**, giving **1** better luminescence performance than **2**. The energy transfer processes in **2** may be similar to those in the $Tb(Benz)_3(phen)$ [19] and TbL'_3 $(DMF)(H_2O)$ ($HL' = p$-aminobenzoic acid) [20], resulting in poorer luminescence of **2** than **1**, even though there are few coordination waters in **2**. This shows that energy transfer from ligand to Tb^{3+} may be more effective, i.e. the energy loss from thermal vibration of the coordinated water in energy transfer is less and serves as experimental evidence for the energy transfer mechanism proposed by Yu and Su for ternary rare earth complexes.

Coordination mode of ligand in a complex is important in matching the lowest triplet state energy level of the ligand to the lowest exited state of Tb^{3+}, which subsequently influences the luminescence property of the complex [4, 20]. Thus, the luminescence performance of **2** should be better than that of **1** from the number of ligands, which coordinate with bidentate chelating carboxylate. However, our result is different. Therefore, we conclude that among the three factors (coordination water, characteristics of the second ligand and ligand coordination mode) that influence the luminescence of a complex, the second ligand is more dominant than the other two, an important conclusion for further research on applications of rare earth complexes with luminescence. Thus, it is worthwhile to further study the effect of the second ligand on the luminescence performance of lanthanide complexes.

4. Conclusions

(a) Complexes **1** and **2** are binuclear with two equivalent structural units corresponding to one half of the dimer, and eight coordination for Tb^{3+} in a distorted square-antiprism.

(b) Two new terbium complexes have been synthesized, structurally characterized and their luminescence performance studied. A coordination water in terbium complexes can be replaced with DMF and the luminescence of the complex is much lower. Less coordination water and more bidentate chelating carboxylates would increase the luminescence intensity of **2**, but DMF as the second ligand in **2** reduces the fluorescence intensity of **2**. Therefore, the characteristics of the second ligand may be an important factor influencing energy transfer between the ligand and the center ion, in turn, influencing the luminescence intensity.

Supplementary material

Crystallographic data for the structural analyses have been deposited with the Cambridge Crystallographic Data Centre, CCDC Nos. 634138 for **1** and 633758 for **2**. Copies of these may be obtained free of charge from: The Director, CCDC, 12 Union Road, Cambridge CB2 1EZ, UK (Fax: +44 1223 336033. E-mail: deposit@ccdc.cam.ac.uk or www: http://www.ccdc.cam.ac.uk).

References

[1] C.H. Huang. *Coordination Chemistry of Rare Earths* [*M*], Science Press, Beijing, 363 (1997).
[2] B.L. An, M.L. Gong, J.M. Zhang, S.L. Zheng. *Polyhedron*, **22**, 2719 (2003).
[3] Y.H. Hou, C.X. Du, Y. Zhu, Z.X. Zhou. *Acta Chim. Sinica*, **61**, 367 (2003).
[4] C.H. Ye, H.L. Sun, XY. Wang, J.R. Li, D.B. Nie, W.F. Fu, S. Gao. *J. Solid State Chemistry*, **177**, 3735 (2004).
[5] X.J. Zheng, L.P. Jin, Z.M. Wang, C.H. Yan, S.Z. Lu, Q. Li. *Polyhedron*, **22**, 323 (2003).
[6] C. Tedeschi, C. Picard, J. Azema, B. Donnadieu, P. Tisnes. *New J. Chem.*, **24**, 735 (2000).
[7] J.G. Mao, T.C.W. Mak, H.J. Zhang, J.Z. Ni, S.B. Wang. *J. Coord. Chem.*, **47**, 145 (1999).
[8] J.G. Mao, H.J. Zhang, J.Z. Ni, S.B. Wang, T.C.W. Mak. *Polyhedron*, **17**, 3999 (1998).
[9] L.G. Zhu, H.P. Xiao. *J. Rare Earths*, **20**, 400 (2002).
[10] S.M. Zheng, L.P. Jin, M.Z. Wang, J.H. Zhang, S.Z. Lu. *Chemical J. Chinese Universities*, **16**, 1007 (1995).
[11] P.R. Selvin, J. Jancarik, M. Li, L.W. Hung. *Inorg. Chem.*, **35**, 700 (1996).
[12] H.Y. Sun, Ch.H. Huang, X.L. Jin, G.X. Xu. *Polyhedron*, **14**, 1201 (1995).
[13] L.P. Jin, S.X. Lu, S.Z. Lu. *Polyhedron*, **15**, 4069 (1996).
[14] D.T. Vodak, M.E. Braun, J. Kim, M. Eddaoudi, O.M. Yaghi. *Chem. Commun.*, 2534 (2001).
[15] B. Yan, Q.Y. Xie. *Inorg. Chem. Commun.*, **6**, 1448 (2003).
[16] B. Yan, Q.Y. Xie. *J. Mol. Struct.*, **688**, 73 (2004).
[17] J. Kay, J.W. Moore, M.D. Glick. *Inorg. Chem.*, **11**, 2818 (1972).
[18] J.W. Moore, M.D. Glick, W.A. Baker. *J. Am. Chem. Soc.*, **94**, 1858 (1972).
[19] X.J. Yu, Q.D. Su. *J. Photochem. Photobiol., A: Chem.*, **155**, 73 (2003).
[20] L. Oyang, H.L. Sun, X.Y. Wang, J.R. Li, Da.B. Nie, W.F. Fu, S. Gao, K.B. Yu. *J. Mol. Struct.*, **740**, 175 (2005).
[21] B. Yan, H.J. Zhang, J.Z. Ni. *Chinese J. Chem.*, **15**, 242 (1997).
[22] H.J. Zhang, B. Yan, S.B. Wang, J.Z. Ni. *J., Photochem. Photobiol., A: Chem.*, **109**, 223 (1997).
[23] B. Yan, H.J. Zhang, J.Z. Ni. *Chinese Chem. Lett.*, **8**, 353 (1997).
[24] B. Yan, H.J. Zhang, S.B. Wang, J.Z. Ni. *Spectrosc. Lett.*, **31**, 603 (1998).
[25] Z.M. Wang, J.R. Cao, H.F. Yang. *J. Shanghai Teachers Univ. (Natural Sciences)*, **25**, 42 (1996).
[26] L.F. Wang, J.G. Wu, Zh.Q. Gao, F.Y. He, X. Gao. *J. Lanzhou Univ. (Natural Sciences)*, **31**, 165 (1995).
[27] X.Y. Zhao, L.F. Wang, J.G. Wu, Zh.Q. Gao. *J. Rare Earth*, **15**, 63 (1994).
[28] B. Wanda, K. Alina. *J. Chem. Res. Synop.*, **1**, 26 (1991).
[29] Y.Sh. Song, B. Yan, Zh.X. Chen. *J. Solid State Chem.*, **177**, 3805 (2004).

[30] B. Yan, Q.Y. Xie. *Inorg. Chem. Commun.*, **6**, 1448 (2003).
[31] H.X. Wu, Z.M. Wang, H.F. Yang, X.B. Yu. *J. Chinese Rare Earth Soc.*, **20**, 289 (2002).
[32] X.H. Yin, M.Y. Tan. *J. Chinese Rare Earth Soc.*, **20**, 240 (2002).
[33] J.J. An, Z.C. Chen. *Chem. Soc. Jpn*, 261 (1986).
[34] H.L. Sun, Ch.H. Ye, X.Y. Wang, J.R. Li, S. Gao, K.B. Yu. *J. Mol. Struct.*, **702**, 77 (2004).
[35] M.C. Yin, Ch.Ch. Ai, L.J. Yuan, Ch.W. Wang, J.T. Sun. *J. Mol. Struct.*, **691**, 33 (2004).